International Journal of Power Electronics and Drive System (IJPEDS)
Vol. 16, No. 4, December 2025, pp. 2186∼2196
ISSN: 2088-8694, DOI: 10.11591/ijpeds.v16.i4.pp2186-2196

Adaptive fuzzy logic controller based BLDC motor to improve the dynamic performance for electric tractor application

Ashwini Yenegur, Mungamuri Sasikala
Department of Electrical and Electronics Engineering, Faculty of Engineering and Technology (Exclusively for Women), Sharnbasva University, Kalaburagi, India

Article Info

Article history:

Received Jan 22, 2025
Revised Aug 18, 2025
Accepted Sep 2, 2025

Keywords:

Adaptive FLC
BLDC motor
Dynamic performance
Electric tractor
MATLAB/Simulink

ABSTRACT

Permanent magnet brushless DC (PMBLDC) motors are widely used in a variety of industrial applications due to their high-power density and ease of regulation. The three-phase power semiconductors bridge is the standard way for controlling these motors. In order to initiate the inverter bridge and switch on the power devices, rotor position sensors must be provided with the correct commutation sequence. The power devices commutate progressively 60 degrees, depending on the location of the rotor. The right speed controllers are necessary for the motor to run as efficiently as possible. PI controllers are commonly employed with permanent magnet motors to achieve speed control in simple manner. Nevertheless, these controllers provide challenges in managing control complexity, including nonlinearity, parametric fluctuations, and load disturbances. PI controllers need accurate linear mathematical models. To overcome this, in this paper adaptive fuzzy logic controller (FLC) for controlling the speed of a BLDC motor is presented. When the motor drive system uses the adaptive FLC technology for speed control, it exhibits better dynamic behavior and is more resistant to changes in parameters and load disturbances. The main objectives of this work are to analyze and appraise the functioning of an electric tractor driven by a PMBLDC motor drive using adaptive FLC. The PMBLDC motor drive controllers are simulated using MATLAB/Simulink software.

Corresponding Author:

Ashwini Yenegur
Department of Electrical and Electronic Engineering
Faculty of Engineering and Technology (Exclusively for Women), Sharnbasva University
Kalaburagi, Karnataka, India
Email: ashwiniyenegur@gmail.com

1. INTRODUCTION

Brushless DC motors are mostly used for rotary, actuation, positioning, and variable speed uses that need to be stable and have accurate motion control. In order to provide continuous control under varied operating conditions, an effective controller must be designed [1]. Due to their fixed gain parameters, classic motor controllers like PI and PID controllers are sensitive to changes in load, speed fluctuations, and parameter variations [2]-[4]. Sliding mode control (SMC)-based algorithms have been investigated by researchers for use in electric drive applications. One of SMC's main shortcomings is that the chattering issues which causes the system's performance to deteriorate. These problems with conventional control algorithms have piqued the curiosity of researchers, who are looking to build and analyze electric motor system controllers using artificial intelligence (AI) methods. They have created AI control methods for speed control, such as neural network approaches and fuzzy logic, as a result of their model-free design philosophy. Several controllers for BLDC motor drives were compared in terms of resilience [5]. Along with conventional fuzzy and ANFIS, self-tuning FLC approaches have also been suggested to make FLC more resilient to outside disturbances [6]. When the motor's parameters change, the system adapts by adjusting the scaling factors, rule base, and membership function of the parameters. A "self-tuning fuzzy logic controller" (FLC) describes this approach [7]. By setting the parameters of membership function (MF), which has a major influence on parameter fluctuations among the different self-tuning methods, this research aims to build a resilient and adaptable controller. Servo, regulatory, and steady-state responses are among the areas the proposed controller's advantages are investigated. Here is the outline of proposed paper: i) Section 2 deals into the mathematical modeling of BLDC and how the BLDC motor driving system works; ii) Section 3 deals with the FLC design and also discusses the proposed controller's adaptive FLC approach; iii) Section 4 validates the simulation results, shows the findings compared to other controllers; and iv) Section 5 gives the conclusion.

2. METHOD

Figure 1 illustrates a speed control system for a BLDC motor used in an electric tractor, employing an adaptive fuzzy logic controller (FLC) for precise speed control. The process begins with a 3-phase AC supply, which is converted to DC through a rectifier [8]. This DC supply is then modulated using a PWM rectifier to provide controlled voltage to the motor.

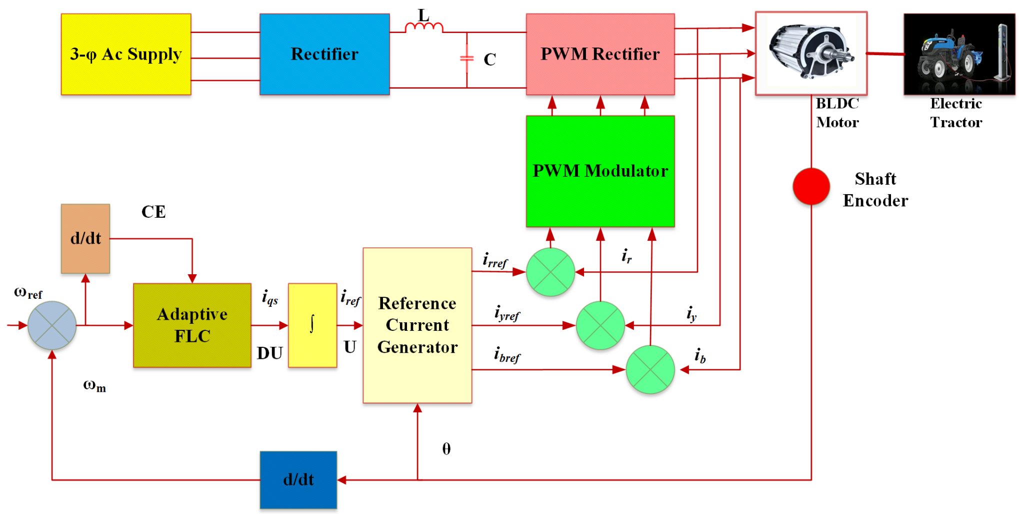

Figure 1. The general configuration of adaptive FLC-based speed control of BLDC motor

The motor's speed is monitored via a shaft encoder, which feeds back the actual speed (ω_m) to the control system. The adaptive FLC compares the actual speed with the reference speed (ω_{ref}) and calculates the error. Based on this error and its rate of change, the FLC adjusts the reference current (i_{ref}). This current is passed through the reference current generator, which generates the appropriate phase currents (i_{rref}, i_{yref}, i_{bref}) to control the motor [9].

The PWM modulator translates these reference currents into switching signals, which are fed into the BLDC motor which will drive the tractor. The entire process is a closed-loop system, with continuous feedback ensuring that the motor operates at the desired speed by adapting to load changes and external disturbances, resulting in smooth and efficient operation [10].

2.1. Modeling of BLDC motor

A permanent magnet with three stator winding makes up the BLDCM rotor. It is possible to disregard currents produced by the rotor due to the high resistance of magnets and stainless steel. There is no damper winding simulation [11]. By solving the circuit equation for the three windings, we get the phase variables.

$$\begin{bmatrix} V_{rst} \\ V_{yst} \\ V_{bst} \end{bmatrix} = \begin{bmatrix} R_{st} & 0 & 0 \\ 0 & R_{st} & 0 \\ 0 & 0 & R_{st} \end{bmatrix} \begin{bmatrix} i_{rst} \\ i_{yst} \\ i_{bst} \end{bmatrix} + \frac{d}{dt} \begin{bmatrix} L_{rr} & L_{ry} & L_{yb} \\ L_{yr} & L_{yy} & L_{yb} \\ L_{br} & L_{by} & L_{bb} \end{bmatrix} \begin{bmatrix} i_{rst} \\ i_{yst} \\ i_{bst} \end{bmatrix} + \begin{bmatrix} e_r \\ e_r \\ e_b \end{bmatrix} \tag{1}$$

Where the stator phase voltages are represented by v_{ast}, v_{bst}, and v_{cst}, and the stator resistance is represented by Rs. The stator's three-phase currents are i_{cst}, i_{ast}, and i_{bst}. Each phase has its own self-inductance, which are L_{aa}, L_{bb}, and L_{cc}. The phase-to-phase inductances are L_{ab}, L_{bc}, and L_{ac}. Phases Ea, Eb, and Ec are associated with electromotive pressures. The resistance of each winding has been assumed to be equal [12]. Furthermore, it is thought that the rotor reluctance does not change with angle because there is no conspicuous rotor.

$$L_{\ rr} = L_{\ yy} \ = L_{\ bb} \ = L \tag{2}$$

$$L_{rr} \ = \ L_{yr} \ = \ L_{rb} \ = \ L_{br} \ = \ L_{yb} \ = \ L_{by} \ = \ M \tag{3}$$

The PMBDCM model is constructed by replacing (1) with (2) and (3).

$$\begin{bmatrix} V_{rst} \\ V_{yst} \\ V_{bst} \end{bmatrix} = \begin{bmatrix} R_{st} & 0 & 0 \\ 0 & R_{st} & 0 \\ 0 & 0 & R_{st} \end{bmatrix} \begin{bmatrix} i_{rst} \\ i_{yst} \\ i_{bst} \end{bmatrix} + \frac{d}{dt} \begin{bmatrix} L & M & M \\ M & L & M \\ M & M & L \end{bmatrix} \begin{bmatrix} i_{rst} \\ i_{yst} \\ i_{bst} \end{bmatrix} + \begin{bmatrix} e_r \\ e_y \\ e_b \end{bmatrix} t \tag{4}$$

The source voltages, which may be thought of as v_{ast}, v_{bst}, and v_{cst}.

$$v_{rst} = v_{ro} - v_{no}, v_{yst} = v_{yo} - v_{no} and v_{bst} = v_{bo} - v_{no} \tag{5}$$

Where v_{no} is the zero-reference potential at the midpoint of dc connection and v_{ro}, v_{yo}, v_{bo}, and v_{no} are the three-phase and neutral voltages, respectively. The stator phase currents are limited to be balanced, as in (6).

$$i_{rst} + i_{yst} + i_{bst} = 0 \tag{6}$$

Because of this, the inductance grid is made easier to understand.

$$M_{iy} + M_{ib} = -M_{ir} \tag{7}$$

Consequently, in the domain of state space, as (8).

$$\begin{bmatrix} V_{ast} \\ V_{bst} \\ V_{cst} \end{bmatrix} = \begin{bmatrix} R_{st} & 0 & 0 \\ 0 & R_{st} & 0 \\ 0 & 0 & R_{st} \end{bmatrix} \begin{bmatrix} i_{ast} \\ i_b st \\ i_{cst} \end{bmatrix} + \frac{d}{dt} \begin{bmatrix} L-M & 0 & 0 \\ 0 & L-M & 0 \\ 0 & 0 & L-M \end{bmatrix} \begin{bmatrix} i_{ast} \\ i_{bst} \\ i_{cst} \end{bmatrix} + \begin{bmatrix} e_a \\ e_b \\ e_c \end{bmatrix} \tag{8}$$

The assumption has been that the back EMFs (e_r, e_y, and e_b) have a trapezoidal wave from (9).

$$\begin{bmatrix} e_r \\ e_y \\ e_b \end{bmatrix} = \omega_m \lambda_m \begin{bmatrix} f_{rs}(\theta_r) \\ f_{ys}(\theta_r) \\ f_{bs}(\theta_r) \end{bmatrix} \tag{9}$$

In this context, ω_m represents the angular rotor speed in rad/sec, m stands for the flux linkage, and r is the rotor position in radians. The functions $f_{rs}(\theta_r)$, $f_{ys}(\theta_r)$ and $f_{bs}(\theta_r)$ are identical to e_r , e_y and e_b, with a maximum magnitude of ±1. Induced emfs don't have sharp corners because they're trapezoidal. A continuous function, electromagnetic fields are generated by the derivatives of flux connections [13]. Because of fringes, the flux density function is smooth and devoid of sharp edges. The electromagnetic toque, according to Newton, is as (10).

$$T_e = e_a i_r + e_b i_y + e_a i_b \tag{10}$$

The inertia is defined as (11).

$$J = J_m + J_l \tag{11}$$

The (12) includes the variables inertia (J), friction coefficient (B), and load torque Tl.

$$J\frac{d\omega_m}{dt} + B\omega_m = (T_e - T_l) \quad (12)$$

The speed-position relationship of the electrical rotor.

$$\frac{d\theta_r}{dt} = \frac{p}{2}\omega_m \quad (13)$$

The damping coefficient B influences the system despite its usually negligible size. Each 2ϕ cycles, the rotor position, represented by the equation "θ_r is repeated. One must take into account the potential of the point of neutrality with regard to zero potential (v_{no}) in order to avoid a voltage imbalance and maintain drive efficiency [14]. By substituting (6) for (8) in the VI equation, we get (14).

$$v_{r0} + v_{y0} + v_{b0} - 3v_{n0} = R_s\left(i_r + i_y + i_b\right) + (L - M)\left(pi_r + pi_y + pi_b\right) + \left(e_r + e_y + e_b\right) \quad (14)$$

Changing (14) to (6) yields the following as (15).

$$v_{r0} + v_{y0} + v_{b0} - 3v_{n0} = \left(e_r + e_y + e_b\right) \quad (15)$$

Thus

$$v_{n0} = [v_{r0} + v_{y0} + v_{b0}] - (e_r + e_y + e_b)]/3 \quad (16)$$

There is a connection between the differential (8), (12), and (13). describes the model by making use of variables that are independent i_{rst},i_{yst},i_{bst},ω_m and θ_r. Combining all relevant equations yields (17)-(23).

$$\dot{x} = Ax + Bu + Ce \quad (17)$$

Where,

$$x = \begin{bmatrix} i_{rst} & i_{yst} & i_{bst} & \omega_m & \theta_r \end{bmatrix}^t \quad (18)$$

$$A = \begin{bmatrix} -\frac{R_{st}}{L-M} & 0 & 0 & -\frac{\lambda_m}{J}f_{rs}(\theta_r) & 0 \\ 0 & -\frac{R_{st}}{L-M} & 0 & -\frac{\lambda_m}{J}f_{ys}(\theta_r) & 0 \\ 0 & 0 & -\frac{R_{st}}{L-M} & -\frac{\lambda_m}{J}f_{bs}(\theta_r) & 0 \\ \frac{\lambda_m}{J}f_{rs}(\theta_r) & \frac{\lambda_m}{J}f_{ys}(\theta_r) & \frac{\lambda_m}{J}f_{bs}(\theta_r) & -\frac{B}{J} & 0 \\ 0 & 0 & 0 & \frac{P}{2} & 0 \end{bmatrix} \quad (19)$$

$$B = \begin{bmatrix} -\frac{1}{L-M} & 0 & 0 & 0 \\ 0 & -\frac{1}{L-M} & 0 & 0 \\ 0 & 0 & -\frac{1}{L-M} & 0 \\ 0 & 0 & 0 & -\frac{1}{L-M} \end{bmatrix} \quad (20)$$

$$C = \begin{bmatrix} -\frac{1}{L-M} & 0 & 0 \\ 0 & -\frac{1}{L-M} & 0 \\ 0 & 0 & -\frac{1}{L-M} \\ 0 & 0 & 0 \end{bmatrix} \quad (21)$$

$$u = \begin{bmatrix} v_{rst} & v_{yst} & v_{bst} & T_l \end{bmatrix}^t \quad (22)$$

$$e = \begin{bmatrix} e_r & e_y & e_b \end{bmatrix}^t \quad (23)$$

A three-phase winding stator and a permanent-magnet rotor characterize a BLDC motor, which is analogous to an induction motor. This gadget has a trapezoidal back emf. When it comes to commutation, the inverter steps in as an electronic commutator by controlling the conduction's switching sequence [15]. To adjust the BLDC motor's speed, one must be aware of its rotor's location. One way to learn this is to use hall effect sensors. The standard configuration for BLDCMs consists of three hall effect sensors spaced by 120 degrees. A high logic state is shown every time the rotor passes the sensor. If not, it will stay in the low logic state. At the end of each cycle, each sensor has completed one full round [16].

The phase voltage changes in relation to the hall sensors' states, and Figure 2(a) demonstrates that the produced back EMF has a trapezoidal shape. In order to spin the rotor, the stator coils are energized by Hall effect sensors that detect its position. Located in Figure 2(b) are the BLDCM's rotor and stator coils. Every sixty degrees, the data is collected from the hall effect sensors. There are six distinct phases to a whole cycle [17], [18]. To keep the motor turning after starting, current flows in a series from the two poles that are opposite to each other. The current flows across two coils simultaneously.

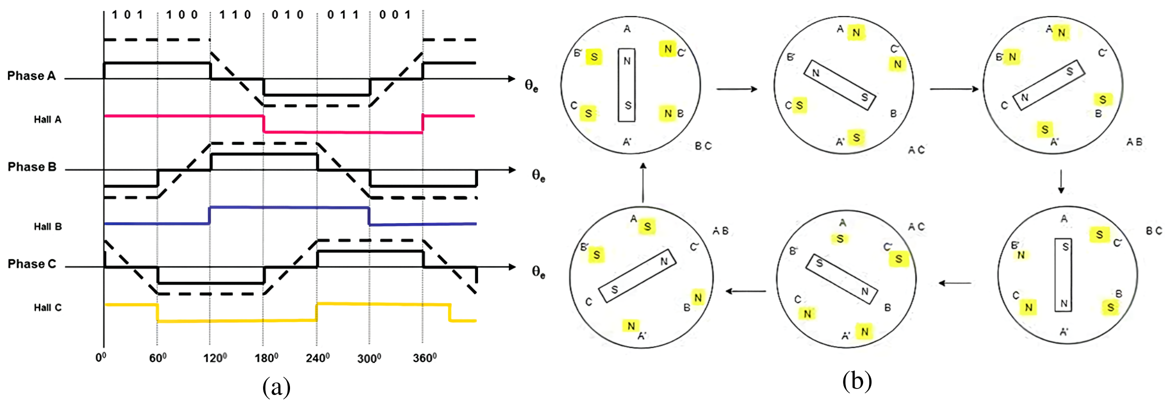

Figure 2. Process of BLDC motor with (a) waveforms of phase and hall sensor signals and (b) six-step commutation process of BLDCM in a sequential manner

3. CONTROL STRATEGY

3.1. Design of conventional FLC

The drive is composed of a BLDC motor, voltage source inverter, hall sensor, fuzzy logic (FL) speed controller, and hysteresis current controller. Two inputs to the FLC are error (e) and change in error (ce), which are expressed as (24) and (25).

$$e(k) = \omega_{ref}(k) - \omega_m(k) \tag{24}$$

$$ce(k) = e(k) - e(k-1) \tag{25}$$

The controller inputs e and ce have membership functions that are defined as [-1, 1] on the normalized domain. To acquire the crisp output, the defuzzification procedure yields the true control output. The available literature indicates that the selection of MF parameters has an impact on FLC performance. Proper tweaking of these factors can enhance FLC's performance [19]. The following section present the ideal tuning mechanism for MF (membership function) parameters. The error $(\omega_r ef - \omega_m)$ serves as the input to the FLC while the changes in the error form the basis for the FLC's operation. Since the FLC continuously measures and calculates the inputs, fuzzy logic rules are employed to modify the PI controller parameters online in order to attain the optimal PI parameters [20]. At different periods, the error and change in error and output may satisfy the PI self-calibration requirements because of the FLC inputs of the adaptive fuzzy PI controller [21]-[23].

Figure 3 shows the block diagram of the fuzzy logic controller. Figure 4 shows the membership functions of the input variables error and change in error, respectively. The membership functions for the proportional gain K_P and the integral gain K_i are developed, as shown in Figure 5, respectively. The flowchart for the recommended control technique is shown in Figure 6.

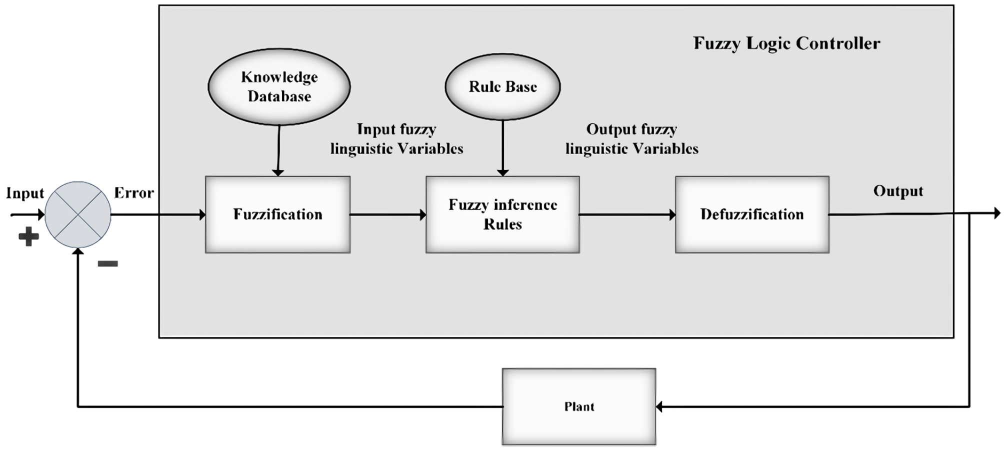

Figure 3. Block diagram of fuzzy logic controller

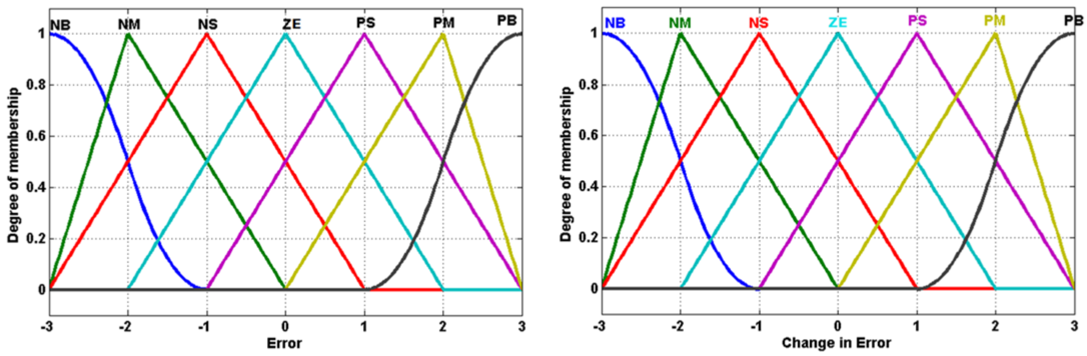

(a) (b)

Figure 4. Membership functions of (a) error and (b) change in error

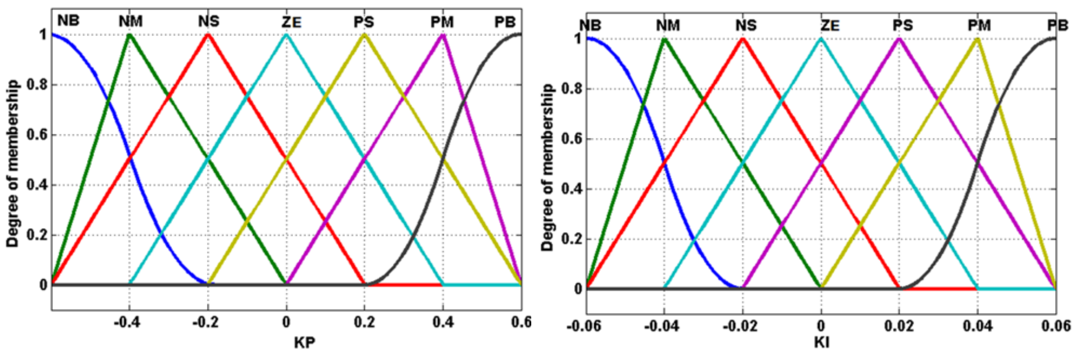

(a) (b)

Figure 5. Membership functions of (a) K_P and (b) K_i

The following are the main properties of fuzzy logic control: Seven triangular membership functions are utilized for both inputs and outputs, fuzzy inference rules number 49, and are 7 by 7. For fuzzification, we employ the continuous universe of discourse, and for implication, we use the "min" operator [24]. Fuzzy implications provide the basis of inference. For defuzzification, the "Centroid" method is employed. The membership functions for all fuzzy variables are negative big (NB), negative medium (NM), negative small (NS), zero (ZE), positive small (PS), positive medium (PM), and positive big (PB) [25].

3.2. Adaptive fuzzy logic controller

The system in Figure 7 is an adaptive fuzzy logic controller for BLDC motor speed control. It combines FLC with a traditional PI controller. The FLC dynamically adjusts the PI controller's gains (Kp and Ki) based on the motor's speed error and rate of change of error, ensuring adaptive tuning. The PI controller uses these adaptive gains to control the motor's speed by adjusting the PWM duty cycle, which regulates the motor's voltage which resulting into a change in speed [25]. This adaptive approach makes the system more robust, improving performance under changing conditions like load variations.

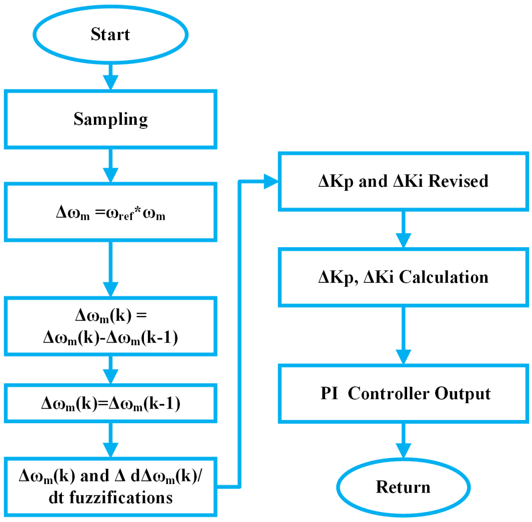

Figure 6. Flowchart

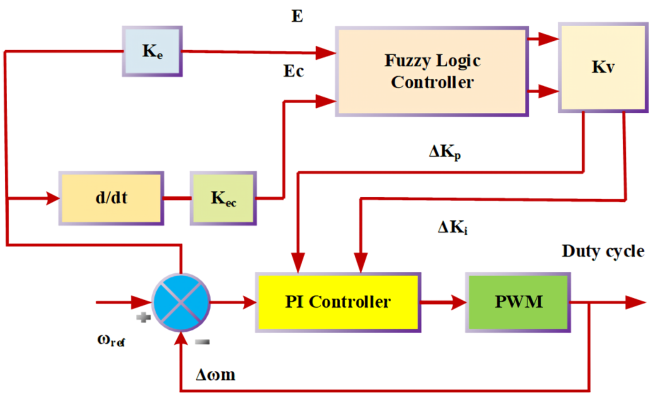

Figure 7. Block diagram of adaptive fuzzy logic controller for BLDC motor

4. RESULTS AND DISCUSSION

4.1. Without load

The speed response of the BLDC motor drive system with FLC is shown in Figure 8(a). It is noticeable that the motor reaches a constant speed of 1000 rpm at 0.4 sec. Figure 8(b) displays the stator voltage and current of the BLDC motor. Stator current stabilizes after 0.1 sec. The waveform shows the back electromotive force of the BLDC motor without a load. The result reveals that the 3-phase back emf voltages are set at 100 V after 0.050 sec. The speed response of the BLDC motor drive system with adaptive FLC is shown in Figure 9(a). It is noticeable that the motor reaches a constant speed of 1000 rpm at a time equals to 0.1 sec.

Figure 9(b) displays the stator voltage and current of the BLDC motor. The stator current stabilizes after 0.2 seconds; the waveforms show the back electromotive force (emf) and current of the BLDC motor without a load. The result reveals that the 3-phase back emf voltages are set at 100 V at time 0.001 sec. Figure

10(a) shows the comparison performances of all suggested controllers for BLDC motors in terms of rise time, settling time, and overshoot percentage. According to Table 1, summary data for the controllers, adaptive FLC has the lowest rise time (0.03 sec), settling time (0.1 sec), and overshoot percentage (8%).

Table 1. comparisons of the dynamic performance of the BLDC motor on no load

S.No.	Controllers	Rise time (msec)	Settling time (msec)	Peak overshoot (%)
1	With PI controller	80	850	15
2	With FLC	70	250	13
3	With Adaptive FLC	30	100	8

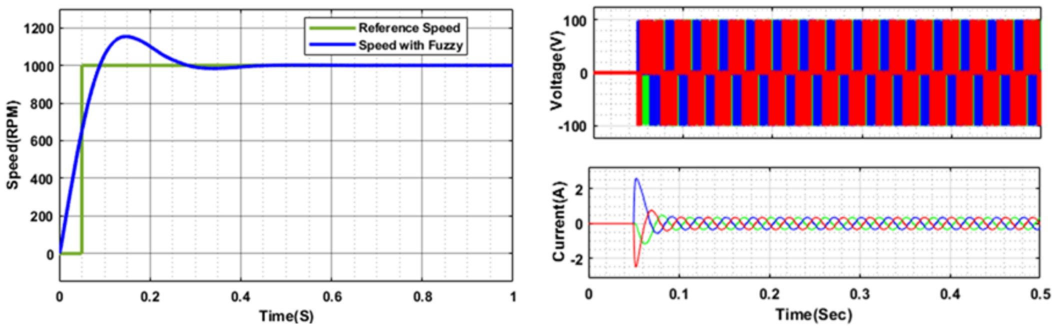

(a) (b)

Figure 8. The results of (a) speed response with FLC and (b) phase voltage and phase current with FLC

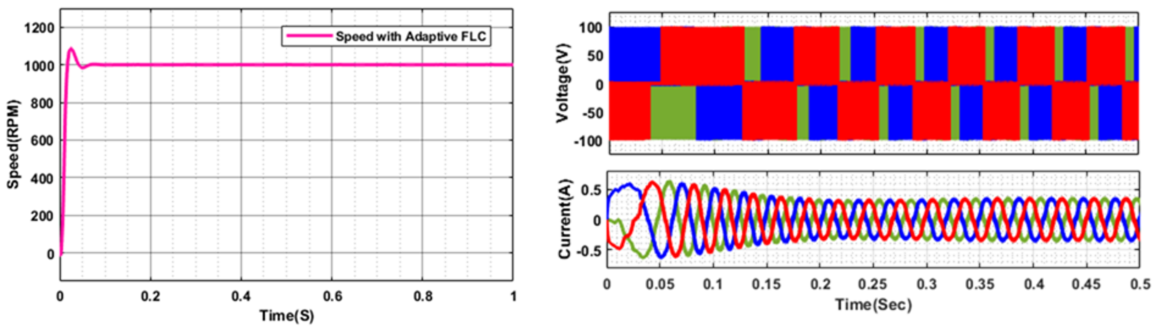

(a) (b)

Figure 9. Results of (a) speed response and (b) phase voltage and current with adaptive FLC

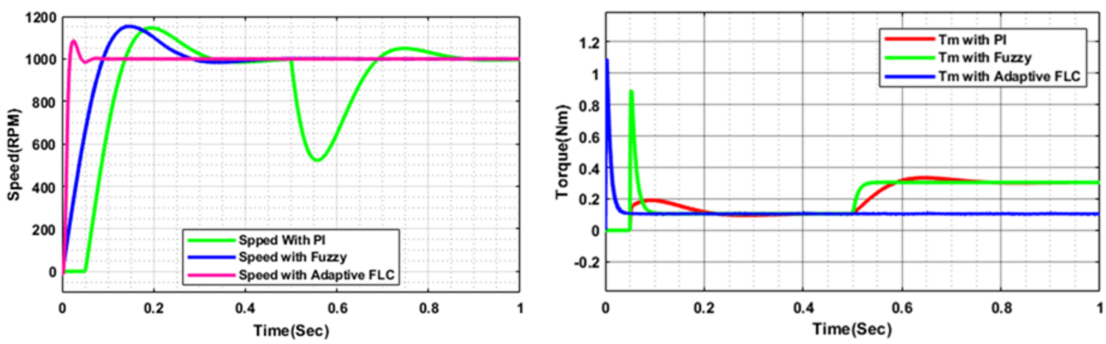

(a) (b)

Figure 10. Variation of (a) speed and (b) torque with FLC and adaptive FLC

The torque responses obtained from the PI, fuzzy logic, and adaptive FL controllers are displayed in Figure 10(b). The torque response of the controller is contingent upon the conditions of the input torque. But then it suddenly slowed down for a split second before heading back to its original position. It has been noted that the torque oscillates less when adaptive FLC is used.

4.2. With 50% load

Figure 11 depicts the BLDC motor's speed at 50% full load. Figure 11 shown the comparison performance of all suggested controllers for the BLDC motor in terms of settling time and overshoot percentage. According to Table 2, summary data for the controllers, adaptive FLC has the lowest settling time (0.18 sec), and overshoot percentage (7.4%). With comparison of fuzzy logic controller and PI controllers, the adaptive FLC gave better performance at 50% of load.

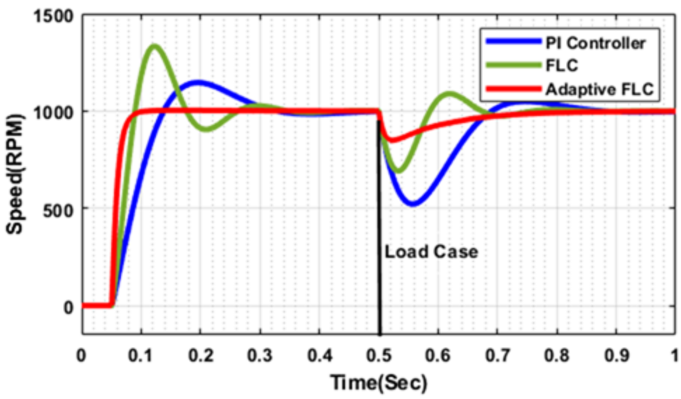

Figure 11. The variation of motor speed with controllers

Table 2. Control performance comparison of BLDC motor at 50% load

S.No.	Controllers	Settling time (msec)	Peak overshoot (%)
1	With PI controller	320	12.5
2	With FLC	280	9.3
3	With adaptive FLC	180	7.4

5. CONCLUSION

The study examines the speed control of a PMBLDC motor using an adaptive fuzzy logic controller and evaluates its effectiveness through modeling and simulation in MATLAB/Simulink. The entire motor drive system was modeled, and its performance was analyzed at different load conditions to assess the controller's ability to control speed efficiently. The results are compared against the performance of the traditional FLC and PI controller. The findings revealed that the adaptive FL controller significantly outperformed both FLC and PI controllers at no load and 50% of full load. Specifically, it provided faster response with decreased rise time, reduced overshoot, and a lower settling time. This highlights the adaptive fuzzy logic controller's superior ability to quickly stabilize the motor speed while maintaining accuracy and efficiency, making it a more effective solution for controlling PMBLDC motors in dynamic environments.

FUNDING INFORMATION

Authors state no funding involved.

AUTHOR CONTRIBUTIONS STATEMENT

This journal uses the Contributor Roles Taxonomy (CRediT) to recognize individual author contributions, reduce authorship disputes, and facilitate collaboration.

Name of Author	C	M	So	Va	Fo	I	R	D	O	E	Vi	Su	P	Fu
Ashwini Yenegur	✓	✓	✓	✓	✓	✓		✓	✓	✓			✓	
Mungamuri Sasikala						✓		✓	✓	✓	✓	✓		

C : **C**onceptualization
M : **M**ethodology
So : **So**ftware
Va : **Va**lidation
Fo : **Fo**rmal Analysis
I : **I**nvestigation
R : **R**esources
D : **D**ata Curation
O : Writing - **O**riginal Draft
E : Writing - Review & **E**diting
Vi : **Vi**sualization
Su : **Su**pervision
P : **P**roject Administration
Fu : **Fu**nding Acquisition

CONFLICT OF INTEREST STATEMENT

Authors state no conflict of interest.

DATA AVAILABILITY

Data availability is not applicable to this paper as no new data were created or analyzed in this study.

REFERENCES

[1] V. Kumarasamy, V. Karumanchetty, Thottam Ramasamy, G. Chandrasekaran, G. Chinnaraj, P. Sivalingam, and N. S. Kumar, "A review of integer order PID and fractional order PID controllers using optimization techniques for speed control of brushless DC motor drive," *International Journal of System Assurance Engineering and Management*, vol. 14, no. 4, pp. 1139–1150, 2023, doi: 10.1007/s13198-023-01952-x.

[2] J. Zhou, S. Ebrahimi, and J. Jatskevich, "Extended operation of brushless DC motors beyond 120° under maximum torque per ampere control," *IEEE Transactions on Energy Conversion*, vol. 38, no. 2, pp. 1280–1291, 2023, doi: 10.1109/TEC.2023.3236594.

[3] B. Divakar, R. K. Naidu, G. Divya, S. Yugandhar, G. M. Deepak, and D. Sindhusha, "A review on brushless DC motor control techniques," *Journal of Pharmaceutical Negative Results*, vol. 13, pp. 6821–6828, 2023, [Online]. Available: https://www.pnrjournal.com/index.php/home/article/view/5930.

[4] X. Li, S. Li, W. Chen, T. Shi, and C. Xia, "A fast diagnosis strategy for inverter open-circuit faults based on the current path of brushless DC motors," *IEEE Transactions on Power Electronics*, vol. 38, no. 8, pp. 9311–9316, 2023, doi: 10.1109/TPEL.2023.3270030.

[5] M. Sundaram, J. Chelladurai, M. Anand, M. S. S. Kumari, S. Sharma, and M. E. H. Assad, "A novel approach to energy-optimized variable-speed sensorless-based brushless DC motors (BLDC) control for automotive wiper applications," *Arabian Journal for Science and Engineering*, vol. 49, no. 2, pp. 1491–1504, 2024, doi: 10.1007/s13369-023-07850-5.

[6] S. Prabhu, V. Arun, M. Balaji, V. Kalaimagal, A. Manikandan, and B. M. Reddy, "Investigations on brushless DC motors for automotive systems," in *Proceedings of the 9th International Conference on Electrical Energy Systems, ICEES 2023*, 2023, pp. 138–142. doi: 10.1109/ICEES57979.2023.10110121.

[7] C. Zhu, R. Lu, C. Mei, T. Peng, and G. Zhang, "Design and simulation analysis of stator slots for small power permanent magnet brushless DC motors," *International Transactions on Electrical Energy Systems*, vol. 2023, 2023, doi: 10.1155/2023/1152243.

[8] C. Luo, J. Wang, E. Zio, and Q. Miao, "Operating condition generalization network for fault diagnosis of brushless DC motors," *IEEE Transactions on Industrial Electronics*, vol. 71, no. 12, pp. 16675–16683, 2024, doi: 10.1109/TIE.2024.3383037.

[9] A. Prakash and C. Naveen, "Combined strategy for tuning sensor-less brushless DC motor using SEPIC converter to reduce torque ripple," *ISA Transactions*, vol. 133, pp. 328–344, 2023, doi: 10.1016/j.isatra.2022.06.045.

[10] D. K. Shary, H. J. Nekad, and M. A. Alawan, "Speed control of brushless DC motors using (conventional, heuristic, and intelligent) methods-based PID controllers," *Indonesian Journal of Electrical Engineering and Computer Science*, vol. 30, no. 3, pp. 1359–1368, 2023, doi: 10.11591/ijeecs.v30.i3.pp1359-1368.

[11] Y. Jouili, R. Garraoui, M. Ben Hamed, and L. Sbita, "Self-adaptive PI-FLC for BLDC motor speed supplied by PEM fuel cell stack optimized by MPPT," *Arabian Journal for Science and Engineering*, vol. 49, no. 5, pp. 6487–6503, 2024, doi: 10.1007/s13369-023-08265-y.

[12] N. L. Manuel, N. İnanç, and M. Lüy, "Control and performance analyses of a DC motor using optimized PIDs and fuzzy logic controller," *Results in Control and Optimization*, vol. 13, p. 100306, 2023, doi: 10.1016/j.rico.2023.100306.

[13] N. A. A. M. Kamal, D. Hanafi, and H. A. Rahman, "Programmable DC motor position using fuzzy logic controller," *Evolution in Electrical and Electronic Engineering*, vol. 4, no. 2, pp. 815–824, 2023, [Online]. Available: http://publisher.uthm.edu.my/periodicals/index.php/eeee.

[14] A. Bahadir and Ö. Aydoğdu, "Modeling of a brushless DC motor driven electric vehicle and its PID-fuzzy control with dSPACE," *Sigma Journal of Engineering and Natural Sciences*, vol. 41, no. 1, pp. 156–177, 2023, doi: 10.14744/sigma.2023.00015.

[15] V. M. Gopala, T. A. Kumar, D. Krishna, C. S. Rao, S. Kumar, and S. Poddar, "Rapid control prototyping of five-level MMC based induction motor drive with different switching frequencies," *EMITTER International Journal of Engineering Technology*, pp. 102–119, Jun. 2022, doi: 10.24003/emitter.v10i1.637.

[16] E. Himabindu, R. Dora, and D. Krishna, "Fuzzy type-II controller based UPQC for power quality enhancement in grid connected micro grid system," in *2022 3rd International Conference for Emerging Technology, INCET 2022*, 2022. doi: 10.1109/INCET54531.2022.9824671.

[17] N. A. Rao and C. R. Kumar, "Speed control of brushless DC motor by using PID and fuzzy logic controller," *International Journal of Innotative Research in Technology (IJIRT)*, vol. 4, no. 6, pp. 72–77, 2019.

[18] E. Himabindu, D. Krishna, and V. M. Gopala, "Performance of intelligent controller-based bearingless switched reluctance motor," *Lecture Notes in Electrical Engineering*, vol. 767, pp. 355–373, 2021, doi: 10.1007/978-981-16-1642-6_28.

[19] T. S. Tamir *et al.*, "Comparative study of four speed controllers of brushless DC motors for industrial applications," *IFAC-PapersOnLine*, vol. 53, no. 5, pp. 59–64, 2020, doi: 10.1016/j.ifacol.2021.04.124.

[20] W. Raza *et al.*, "Fuzzy logic speed regulator for DC motor tuning," *Jurnal Teori dan Aplikasi Matematika (JTAM)*, vol. 8, no. 1, p. 36, 2024, doi: 10.31764/jtam.v8i1.16919.

[21] M. Megrini, A. Gaga, and Y. Mehdaoui, "Sensored brushless DC motor control based on an artificial neural network controller," in *Lecture Notes in Networks and Systems*, 2024, pp. 46–51. doi: 10.1007/978-3-031-48465-0_7.

[22] J. B. S. Freitas, L. Marquezan, P. J. D. de Oliveira Evald, E. A. G. Peñaloza, and M. M. H. Cely, "A fuzzy-based predictive PID for DC motor speed control," *International Journal of Dynamics and Control*, vol. 12, no. 7, pp. 2511–2521, 2024, doi: 10.1007/s40435-023-01368-2.

[23] N. N. Ab Rahman, N. M. Yahya, and N. U. M. Sabari, "Design of a fuzzy logic proportional integral derivative controller of direct current motor speed control," *IAES International Journal of Robotics and Automation*, vol. 12, no. 1, pp. 98–107, 2023, doi: 10.11591/ijra.v12i1.pp98-107.

[24] R. Subbulakshmy, R. Palanisamy, S. Alshahrani, and C. A. Saleel, "Implementation of non-isolated high gain interleaved DC-DC converter for fuel cell electric vehicle using ANN-based MPPT controller," *Sustainability (Switzerland)*, vol. 16, no. 3, p. 1335, 2024, doi: 10.3390/su16031335.

[25] K. V. Gopan and J. D. Shree, "Analysis of bridge type and bridgeless cuk converter fed motor drives for improved power quality," *International Journal of Electronics*, vol. 110, no. 7, pp. 1179–1212, 2023, doi: 10.1080/00207217.2022.2121427.

BIOGRAPHIES OF AUTHORS

Ashwini Yenegur received a B.E. in Electrical and Electronics Engineering from Visvesvaraya Technological University (VTU) in 2012, followed by an M.Tech. in Computer Science and Engineering from the same university in 2014. Currently serving as an assistant professor since 2014 and a research scholar at Sharnbasva University. Research interests focus on power systems, electric drives, intelligent control systems, and renewable energy applications. Actively engaged in national and international conferences, with multiple research papers published in reputed proceedings. Holds memberships in the Board of Studies (BoS) and the Institution of Electronics and Telecommunication Engineers (IETE), contributing to academic and research advancements in the field. She can be contacted at email: ashwiniyenegur@gmail.com.

Mungamuri Sasikala received a B.E. in Electrical Engineering from University College of Engineering, Osmania University, Hyderabad, in 1985 with First Class Distinction, followed by an M.E. in Power Systems from the same institution in 1987, earning a Gold Medal for securing the top rank in the university. Completed a Ph.D. in Electrical Engineering from Jawaharlal Nehru Technological University (JNTU), Hyderabad, in 2008. With over 32 years of teaching and research experience, academic roles have included serving as Professor and Principal in various institutions since 2008, currently associated with Sharnbasva University, Kalaburagi, since 2014. Research interests include power systems, electric drives, intelligent control systems, and renewable energy applications. Published 55 research papers in reputed national and international journals and presented 26 papers at conferences in India and abroad. Successfully guided seven Ph.D. candidates, with four more currently under supervision. Contributions extend to serving as a Reviewer for several international journals, editing a book chapter, and actively participating as a Board of Studies (BOS) and Board of Examiners (BOE) member, an Academic Council Member at Sharnbasva University, and a Doctoral Committee Member for multiple universities. Additionally, served as an Advisor for the UPSC examination. She can be contacted at email: sasi_mun@rediffmail.com.